Original Article

JHSMR Journal of Health Science and Medical Research

Comparative Accuracy of Qualitative and Quantitative Contrast-Enhanced CT Analysis in Differentiating Intrahepatic Mass-Forming Cholangiocarcinoma from Colorectal Liver Metastasis

Nichakarn Sirivichayakul, M.D.[1,2], Thitinan Chulroek, M.D.[1], Sasiprang kongboonvijit, M.D.[1], Napatsa Yimpraphan, RT.[3]

[1]Department of Diagnostic Radiology, Faculty of Medicine, Chulalongkorn University and King Chulalongkorn Memorial Hospital, Bangkok 10330, Thailand.

[2]Department of Diagnostic Radiology, Bhumibol Adulyadej Hospital RTAF, Bangkok 10220, Thailand.

[3]Department of Diagnostic Radiology, King Chulalongkorn Memorial Hospital, Bangkok 10330, Thailand.

Received 19 September 2024 ● Revised 25 October 2024 ● Accepted 1 November 2024 ● Published online 26 March 2025

Abstract:

Objective: To compare the diagnostic performance of qualitative and quantitative computed tomography in differentiating intrahepatic mass-forming cholangiocarcinoma (IHMCC) from colorectal liver metastasis (CRLM).

Material and Methods: A retrospective study analyzed 79 patients (IHMCC n=41, CRLM n=38). Two abdominal radiologists separately reviewed the following parameters: size, location, number, margin, calcification, hepatic capsular retraction, peripheral bile duct dilatation, proximal bile duct enhancement, extrahepatic spreading, regional lymph node enlargement, vascular and adjacent organ invasion, arterial and delayed enhancement. For the quantitative study, regions of interest were placed on lesions and adjacent liver in the non-contrast, portovenous and delayed phases. The percentage attenuation ratio, absolute percentage delayed enhancement, and the enhancement ratio on the portal venous and delayed phases (ERPV and ERD) were calculated. Multivariate logistic regression was used to determine the significant factors.

Results: Ten qualitative features showed statistically significant differences. Satellite lesions (p-value<0.001), right hepatic lobe location (p-value=0.009), irregular margin (p-value=0.028), hepatic capsular retraction (p-value<0.001), peripheral bile duct dilatation (p-value<0.001), proximal bile duct enhancement (p-value=0.002), extrahepatic spreading (p-value=0.002), regional lymph node enlargement (p-value<0.001), vascular invasion (p-value<0.001), and adjacent organ invasion (p-value=0.01) were found more often in IHMCC versus CRLM. For quantitative analysis, size, ERPV,

Contact: Thitinan Chulroek, M.D.
Department of Diagnostic Radiology, Faculty of Medicine, Chulalongkorn University and King Chulalongkorn Memorial Hospital, Bangkok 10330, Thailand.
E-mail: thitinan.c@chula.ac.th

J Health Sci Med Res
doi: 10.31584/jhsmr.20251182
www.jhsmr.org

and ERD showed statistically significant differences (p-value=0.003 and p-value=0.001). Peripheral duct dilatation (OR 21.1,95% CI 5.07,77.7), regional node enlargement (OR 5.8, 95% CI 1.32, 26.085) and ERD (OR 4.4, 95% CI 1.02, 6.54) were significant predictors on multivariate analysis. From the ROC curve, an optimal cut-off of ERD was 0.79 (AUC0.704, 95% CI 0.59, 0.818).

Conclusion: Peripheral bile duct dilatation, regional lymph node enlargement, and ERD greater than 0.79 can be useful in differentiating IHMCC from CRLM.

Keywords: colorectal liver metastasis, delayed enhancement, mass-forming cholangiocarcinoma, multiphase CT, quantitative analysis

Introduction

Cholangiocarcinoma (CCA) arising from biliary epithelium is the second most common primary liver cancer after hepatocellular carcinoma, comprising approximately 10%-15% of all primary liver cancers[1]. CCAs are anatomically classified into intrahepatic and extrahepatic types[2]. Intrahepatic mass-forming cholangiocarcinoma (IHMCC) is the most common subtype of intrahepatic CCA[3]. The prevalence of CCA is high in parts of Southeast Asia, especially northeastern Thailand[4]. CCA is a malignancy with poor overall survival and high mortality rates[5,6].

One of the non-invasive diagnostic modalities of choice to diagnose CCA is multiphase abdominal computed tomography (CT) in the non-contrast, arterial, portal venous, and delayed phases. CT imaging is a widely used modality with several advantages, including high-resolution images, rapid acquisition, and a broad range of clinical applications. Multiphase abdominal CT helps with the diagnosis and treatment planning of CCA[7,8]. Typical imaging characteristics of intrahepatic mass-forming cholangiocarcinoma (IHMCC) on the non-contrast-enhanced CT usually present as a homogeneous or heterogeneous low-attenuating mass. Following the administration of contrast media, the tumor typically exhibits irregular peripheral arterial enhancement, with only minor enhancement observed in the central region of the tumor[9]. The mass becomes hyperattenuating from the portal venous to the delayed phases, relative to normal hepatic parenchyma[10]. Additional findings such as capsular retraction and dilatation of the bile ducts distal to the mass are also typical[7–9,11].

Currently, the incidence of colorectal cancer (CRC) is on the rise, making it one of the most prevalent cancers globally. The liver is the most common organ of distant metastasis in colorectal cancer, affecting 15–25% of CRC patients who present with distant metastases at the time of the primary diagnosis[12]. Contrast-enhanced CT scan is useful imaging for localizing and evaluating lymphovascular invasion, which will affect treatment planning. The radiographic findings in CT imaging can mimic IHMCC. CRLM are typically hypovascular, but arterial-phase scans may increase lesion conspicuity in some cases and may show peripheral rim enhancement with low attenuation center from tumor necrosis[13–15]. Additionally, delayed enhancement may also be present due to the desmoplastic reaction[16].

The differentiation of liver metastases from colorectal adenocarcinoma and IHMCC is difficult, even in histopathology[17]. Most studies have been subjective, descriptive assessments of the findings in CT imaging of those 2 cancers[15]. Therefore, the aim of this study was to

conduct quantitative measurements of delayed enhanced CT imaging in order to differentiate between IHMCC and CRLM. Additionally, we compared the accuracy of these quantitative measurements to those of qualitative analysis.

Material and Methods

Patients

The study obtained ethical approval from the Institutional Review Board of our institute. The requirement of informed consent was waived due to the retrospective design. We searched the list of patients who were diagnosed with cholangiocarcinoma and colorectal liver metastasis from the ICD-10 between January 2015 and February 2020. A total of 1,239 cases with CCA and 2,275 cases with CRLM were identified. The inclusion criteria were patients who underwent abdominal contrast-enhanced CT, including the pre-contrast, arterial, portal venous, and delayed 5-minute phases with a pathology diagnosis of IHMCC and adenocarcinoma with a history of colorectal cancer. From these criteria, we included 113 patients with IHMCC and 102 patients with CRLM. Seventy-two patients of IHMCC were excluded due to a history of previous treatment before CT imaging, such as biliary stent insertion or percutaneous transhepatic biliary drainage that made for streaking artifacts to the lesions (n=67), and the lesions were too small (<1 cm, n=5). Conversely, 64 patients of CRLM were excluded due to a history of other cancers that may have been confounding to the diagnosis of liver metastasis origin (n=4), history of previous treatment before CT imaging (n=38), and poor imaging quality, or the lesions were too small (<1 cm, n=22). In the end, we recruited 41 cases of IHMCC and 38 cases of CRLM.

CT Techniques

In our institution, after 6-hour fasting, the CT scans were performed on a 64-multidetector CT scanner (Discovery CT750 HD; GE HealthCare, USA) with the following parameters: collimation 64x0.625 mm; pitch 1.375; rotation time 0.5 sec; tube voltage 120 kVp; maximum allowable tube current set at 200 mAs on an automated dose reduction system and a 128-multidetector CT scanner (Somatom Definition Flash; Siemens Healthcare, Forcheim, Germany) with the following parameters: collimation 128x0.6 mm; rotation time 0.5 sec; tube voltage 100 kVp; the maximum allowable tube current set 150 mAs on an automated dose reduction system.

All patients underwent the pre-contrast, portal venous, and delayed 5-minute phases. Depending on a patient's size and the CT protocols, the estimated volume of contrast administration used was about 2 mL/kg in most abdominal CT protocols, not exceeding 100-120 mL/dose. Therefore, a bolus of 100-120 mL of Iobitridol (Xenetix 300) was intravenously injected at a rate of 2-3 mL/sec through 18 or 20 gauge.

The sequences and acquisition parameters of all the studies included arterial phase (AP) images, which were obtained at 20–40 seconds, portal venous phase (PVP) images, which were obtained at 70–100 seconds, and the delayed 5-minute phase.

Image interpretation

CT images were reviewed separately by 2 abdominal radiologists who had 8 and 2 years of experience in abdominal imaging using the Picture Archiving and Communication System (PACS, AGFA Impax; AGFA Technical Imaging Systems, Ridgefield Park, NJ, USA). The reviewers were blinded to the pathologic information; however, they were aware that the patients had IHMCC or CRLM. The index lesion, identified as the largest lesion on a single axial image, was used for qualitative and quantitative analysis and gave the presumed diagnosis of each patient. Any disagreements were resolved by a consensus review.

Quantitative image analysis

For quantitative image analysis, the first observer recorded the maximum lesion size of the index lesion on PVP. Each radiologist drew the best-fit region of interest (ROI) on the index lesion at the maximal enhancement area on PVP and the delayed 5-minute phase, as well as the corresponding area on the pre-contrast phase, while avoiding the necrotic and vascular areas. The ROI was also placed in non-tumoral liver parenchyma on the PVP and the delayed 5-minute phase, avoiding vessels. In all cases, the ROI sizes were greater than 1 cm^2. An example of ROI placement is shown in Figure 1. Next, we compared the ratio of enhancement with the following equations:

$$\text{Percentage attenuation ratio (PAR)} = 100 \times \left(\frac{LA_D}{AA_D} - \frac{LA_{PV}}{AA_{PV}}\right)$$

$$\text{Absolute percentage delayed enhancement (APDE)} = 100 \times \left(\frac{LA_{D-}\ LA_{PV}}{LA_D - LA_{NC}}\right)$$

$$\text{Enhancement ratio on PV (ERPV)} = \frac{(LA_{PV} - LA_{NC})}{LA_{NC}}$$

$$\text{Enhancement ratio on D (ERD)} = \frac{(LA_D - LA_{NC})}{LA_{NC}}$$

LA=Lesion attenuation AA=Adjacent liver attenuation
NC=Non-contrast phase PV=Portal venous phase
D=Delayed phase

Qualitative image analysis

Two abdominal radiologists independently reviewed the CT imaging findings using PACS. On PVP, they recorded the location of all the lesions located in the right/left or both hepatic lobes and the number of the lesion as single or multiple, then characterized multiple lesions regarding whether they were satellite lesions (multiple lesions with small nodules surrounding the large one) or separate lesions (multiple liver lesions with similar diameters). The observers then recorded the margins of the index lesions (the largest lesion on a single axial image, selected by the main observer). The tumor margins were categorized as smooth (the edges of the tumor are clearly distinct from the surrounding liver tissue), irregular (the tumor edges are uneven, jagged, or have projections into the surrounding tissue), or ill-defined (the edges of the tumor blend into the surrounding liver tissue). Additionally, they noted the presence or absence of ancillary findings, including arterial enhancement, delayed enhancement, internal calcification (in any lesion), hepatic capsular retraction (defined as focal

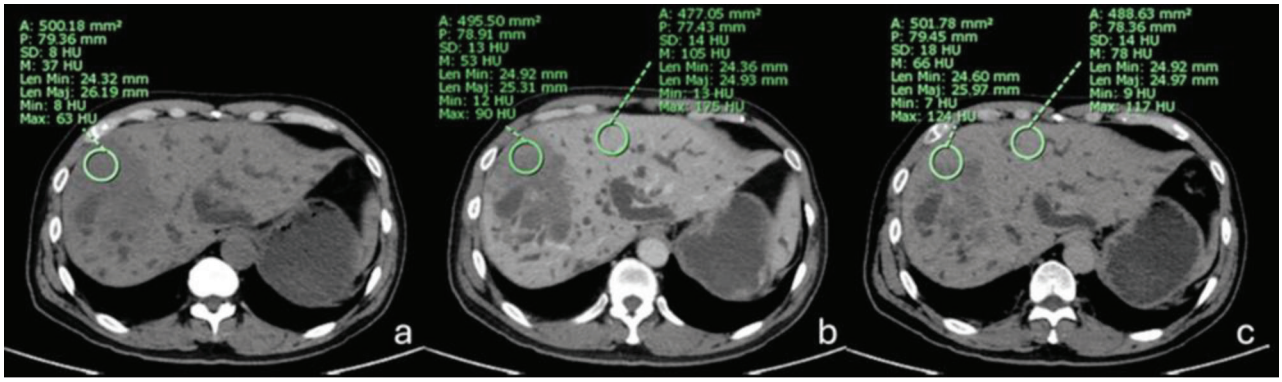

Figure 1 Examples of ROI placement for lesion attenuation are shown in the non-contrast phase (a), lesion and adjacent liver attenuation avoiding vessels in the portal venous phase (b), and in the delayed phase (c)

irregularity, flattening, or concavity of the liver capsule immediately superficial to any liver lesions), vascular invasion (presence of enhancing tumor thrombus within the portal and/or hepatic veins, vascular encasement, or distortion), peripheral bile duct dilatation, proximal bile duct enhancement, extrahepatic spreading (nearby peritoneal nodules or soft tissue, considered to be caused by the liver lesions), regional lymph node enlargement (an enlarged nearby lymph node with a diameter greater than 1.0 cm in the short axis), and adjacent organ invasion (e.g., diaphragm, kidney, adrenal gland)[15,18].

Statistical analysis

Statistical analysis was performed using SPSS version 28. The independent t-test was used to compare the continuous data of the patients' characteristics and CT findings between both groups. Meanwhile, the chi-square test was used to compare categorical variables between both groups. The significant CT findings for differentiating these 2 groups in univariate and multivariate analysis were entered into the logistic regression analysis. The Kappa statistic[19] and intraclass correlation[20] were calculated to assess the interobserver agreement. ROC curve analysis was used to find the optimal cut-off. A p-value of less than 0.05 was considered statistically significant.

Results

Seventy-nine patients were included in this study (48 males and 31 females; mean age 62.8±13.1 years). The IHMCC group consisted of 23 males and 18 females with a mean age of 66.1±11.9 years and the CRLM group consisted of 25 males and 13 females with a mean age of 59.2±13.6 years. The mean age of the IHMCC group was significantly higher than the CRLM group (p-value=0.019). Most of the patients in the IHMCC group were pathologic diagnosed by core needle biopsy while most patients in the CRLM group were diagnosed by surgical biopsy (wedge resection, segmentectomy or lobectomy) (p-value<0.001). For interobserver agreement, there was excellent agreement in all qualitative findings (Kappa=0.76-1.0), whereas good to excellent interobserver agreement in the quantitative analysis (ICC=0.7-0.95). The measurement of tumor density in Hounsfield Units (HU) on the pre-contrast phase had the least agreement (ICC=0.7). The mean size of the index lesions in the IHMCC group was significantly larger than in the CRLM group (87.8 mm vs. 59.42 mm) (p-value=0.004). All clinical characteristics of the patients are shown in Table 1.

Qualitative analysis

We observed 14 features as described in the methods. Ten features showed statistically significant differences between the 2 groups, which consisted of satellite lesions (p-value<0.001), location (p-value=0.009), margin (p-value=0.028), hepatic capsular retraction (p-value<0.001), vascular invasion (p-value<0.001), peripheral bile duct dilatation (p-value<0.001), proximal bile duct enhancement (p-value=0.02), extrahepatic spreading (p-value=0.02), regional lymph node enlargement (p-value<0.001), and adjacent organ invasion (p-value=0.01). The number of lesions, internal calcification, the presence of arterial and delayed enhancement showed no significant differences between the IHMCC and CRLM groups. The details of the qualitative analysis are demonstrated in Table 2. The important CT findings for IHMCC and CRLM are demonstrated in Figure 2 and 3.

Quantitative analysis

There were 4 formulas compared between these 2 groups, including PAR, APDE, ERPV, and ERD. The means of ERPV and ERD showed statistically significant differences between the IHMCC group and the CRLM group (p-value=0.003 and p-value=0.001, respectively). From the ROC analysis, the optimal cut-off of ERPV was 0.72 with a sensitivity and specificity of 48.8% and 73.7%, respectively.

The optimal cut-off of ERD was 0.79 with a sensitivity and specificity of 51.2% and 71.1%, respectively. The results of the quantitative analysis are presented in Table 3.

Logistic regression analysis

By univariate logistic regression analysis, the IHMCC group was predicted by size (p-value=0.006), satellite lesion (p-value<0.001), location in the right hepatic lobe (p-value=0.014), hepatic capsular retraction (p-value<0.001), peripheral bile duct dilatation (p-value<0.001), proximal bile duct enhancement (p-value<0.001), vascular invasion (p-value<0.001), extrahepatic spreading (p-value=0.002), regional lymph node enlargement (p-value<0.001), adjacent organ invasion (p-value=0.009), ERPV with a cut-off of 0.72 (p-value=0.04), and ERD with a cut-off of 0.79 (p-value=0.04). The peripheral bile duct dilatation, regional lymph node enlargement, and ERD remained significant predictors in multivariate analysis, as shown in Table 4.

Diagnostic test

Among the qualitative findings, satellite lesions and peripheral bile duct dilatation had the highest accuracy rates at 84.8% and 82.3%, respectively. The accuracy of the optimum enhancement ratio on PVP and the delayed phases was approximately 60.8%. The diagnostic performance of significant CT findings is demonstrated in Table 5.

Table 1 Clinical characteristics of 2 groups of participants

Characteristics	IHMCC (n=41)	CRLM (n=38)	p-value
Gender			
Male	23 (56.1)	25 (65.8)	0.515
Female	18 (43.9)	13 (34.2)	
Age (years)			
Mean age±S.D.	66.1±11.9	59.2±13.6	0.019*
Range	28-88	35-82	
Pathology method			
Biopsy	31 (75.6)	7 (18.4)	<0.001*
Surgery	10 (24.4)	31 (81.6)	
Pathologic tumor grade (Adenocarcinoma)			
Well differentiated	12 (29.3)	1 (2.6)	
Moderately differentiated	18 (43.9)	5 (13.2)	<0.001*
Poorly differentiated	6 (14.6)	0 (0.0)	
No grading	5 (12.2)	32 (84.2)	
CA 19-9 (U/ml)			
Mean±S.D.	1948.0±8754.2	82.89±134.979	
Range	0.7-42111	3.6-394	0.260
High	23	6	
Normal (0-37)	13	1	
Unknown	5	31	
CEA (ng/ml)			
Mean±S.D.	128.25±465.1	868.35±2670.42	
Range	1.41-2559	1.29-13638	0.529
High	23	29	
Normal (0-5)	5	4	
Unknown	13	5	

Data are the number of patients with percentages in parentheses. *Statistically significant
CA19-9=Cancer Antigen 19-9, CEA=Carcinoembryonic Antigen, IHMCC=intrahepatic mass-forming cholangiocarcinoma, CRLM=colorectal liver metastasis

Table 2 Comparison of the qualitative imaging variables between IHMCC and CRLM

CT Findings	IHMCC (n=41)	CRLM (n=38)	p-value
Number of lesions			
Single	18	15	0.865
Multiple	23	23	
Satellite	18	2	<0.001*
Separate	5	21	
Location			
Right	29	14	0.009*
Left	3	8	
Both	9	16	
Margin			
Smooth	9	16	0.028*
Irregular	24	11	
Ill-defined	8	11	
Internal calcification			
Yes	9	11	0.649
No	32	27	
Hepatic capsular retraction			
Yes	25	7	<0.001*
No	16	31	
Vascular invasion			
Yes	32	9	<0.001*
No	9	29	
Peripheral bile duct dilatation			
Yes	33	6	<0.001*
No	8	32	
Proximal bile duct enhancement			
Yes	19	5	0.002*
No	21	33	
Extrahepatic spreading			
Yes	17	3	0.002*
No	24	35	
Regional lymph node enlargement			
Yes	23	5	<0.001*
No	18	33	
Adjacent organ invasion			
Yes	14	3	0.01*
No	27	35	
Arterial enhancement			
Yes	23	15	0.423
No	18	19	
Delayed enhancement			
Yes	38	33	0.627
No	3	5	

*Statistically significant
IHMCC=intrahepatic mass-forming cholangiocarcinoma, CRLM=colorectal liver metastasis

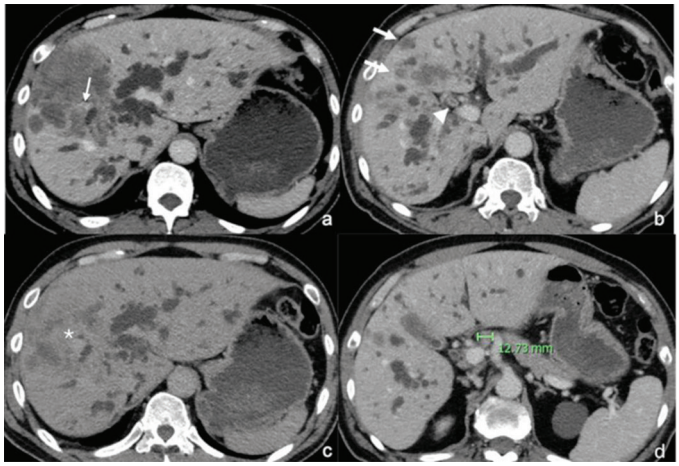

IHMCC=intrahepatic mass-forming cholangiocarcinoma, ERPV=enhancement ratio on the portal venous phase, ERD=enhancement ratio on the delayed phase

Figure 2 A case of a 60-year-old male with a pathological diagnosis of IHMCC (moderately differentiated adenocarcinoma). (a) Multiphase contrast-enhanced computed tomography shows a large irregular hypoenhancing mass in the right hepatic lobe on the portovenous phase with vascular encasement (arrow). (b) The lower level shows multiple surrounding small nodules (satellite lesions, arrows) with peripheral bile duct dilatation and common bile duct enhancement (arrowhead). (c) The 5-minute delayed phase shows increased centripetal delayed enhancement, particularly in the central area (asterisk). (d) There is an enlarged hepatoduodenal lymph node, about 1.3 cm in short axis. The ERPV was 0.76 and the ERD was 0.85, which is more than the optimal cut-off for IHMCC

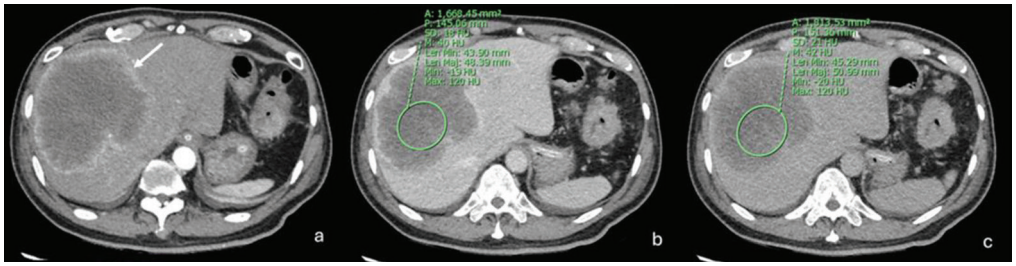

CA19-9=Cancer Antigen 19-9, CEA=Carcinoembryonic Antigen, ERPV=enhancement ratio on the portal venous phase, ERD=enhancement ratio on the delayed phase

Figure 3 A case of 65-year-old male with pathological diagnosis of colorectal liver metastasis. CA19-9 >1000 U/ml and CEA 206 ng/ml. The multiphase contrast-enhanced computed tomography shows a single 13.2-cm mass in the right hepatic lobe. (a) The arterial phase image shows peripheral hepatic enhancement (arrow). (b) The portovenous phase shows thin peripheral enhancement with smooth margin. (c) The 5-minute delayed phase shows increased enhancement based on the visual qualitative assessment. No other findings, such as hepatic capsular retraction, peripheral bile duct dilatation or regional node enlargement, were observed. The ERPV and ERD were 0.36 and 0.40, respectively

Table 3 Comparison of the quantitative imaging variables between IHMCC and CRLM

CT Findings (Quantitative)	IHMCC (n=41)	CRLM (n=38)	p-value
Size (mm.)			
Mean (S.D.)	87.8 (38.86)	59.42 (46.65)	0.004*
PAR			
Mean (S.D.)	19.5578 (10.73)	18.9 (8.35)	0.898
APDE			
Mean (S.D.)	1.39 (30.9)	-1.02 (43.67)	0.534
ERPV			
Mean (S.D.)	0.87 (0.42)	0.61 (0.33)	0.003*
ERD			
Mean (S.D.)	0.92 (0.44)	0.64 (0.31)	0.001*

*Statistically significant
IHMCC=intrahepatic mass-forming cholangiocarcinoma, CRLM=colorectal liver metastasis, mm.=millimeter, S.D.=standard deviation, PAR=percentage attenuation ratio, APDE=absolute percentage delayed enhancement, ERPV=enhancement ratio on the portal venous phase, ERD=enhancement ratio on the delayed phase

Table 4 Univariate and multivariate logistic regression analysis of CT findings for diagnosing IHMCC

CT Findings	Univariate analysis		Multivariate analysis	
	p-value	OR	p-value	aOR
Number of lesions	0.69	0.83	-	-
Satellite/Separate	<0.001*	37.8	-	-
Location in right hepatic lobe	0.014*	3.68	-	-
Margin (irregular)	0.014*	3.879	-	-
Internal calcification	0.48	0.69	-	-
Hepatic capsular retraction	<0.001*	6.92	-	-
Vascular invasion	<0.001*	11.46	-	-
Peripheral bile duct dilatation	<0.001*	22.0	<0.001*	21.1
Proximal bile duct enhancement	<0.001*	5.9	-	-
Extrahepatic spreading	0.002*	8.26	-	-
Regional lymph node enlargement	<0.001*	8.4	0.024*	5.84
Adjacent organ invasion	0.009*	6.05	-	-
Arterial enhancement	0.302	1.62	-	-
Delayed enhancement	0.40	1.9	-	-
Size	0.006*	1.1	-	-
PAR	0.89	0.99	-	-
APDE	0.53	1.002	-	-
ERPV (cut-off=0.72)	0.042*	2.67	-	-
ERD (cut-off=0.79)	0.042*	2.58	0.035*	4.42

*Statistically significant
Dash (-) indicates not significant on multivariate analysis, IHMCC=intrahepatic mass-forming cholangiocarcinoma, CT=computed tomography, OR=odds ratio, aOR=adjust odds ratio, PAR=percentage attenuation ratio, APDE=absolute percentage delayed enhancement, ERPV=enhancement ratio on the portal venous phase, ERD=enhancement ratio on the delayed phase

Table 5 The diagnostic performance of each significant CT finding in diagnosing IHMCC, utilizing the best cut-offs for statistically significant quantitative findings

CT findings	Sensitivity	Specificity	PPV	NPV	Accuracy
Qualitative variables					
Satellite lesions	78.3 [61.4-95.12]	91.3 [79.80-102.8]	90.0 [76.9-103.12]	80.8 [65.6-95.92]	84.8 [74.5-95.1]
Right lobe location	72.5 [58.6-86.34]	63.2 [47.8-78.4]	67.4 [53.4-81.4]	68.6 [53.2-83.6]	67.0 [56.6-77.4]
Irregular margin	58.5 [43.5-73.6]	71.1 [56.6-85.5]	68.6 [53.2-83.4]	61.4 [46.9-75.6]	64.6 [54.1-75.14]
Hepatic capsular retraction	60.9 [46.0-75.9]	81.6 [69.3-93.9]	78.1 [63.8-92.4]	65.96 [52.4-79.5]	70.9 [60.9-80.9]
Vascular invasion	78.0 [65.4-90.7]	76.3 [62.8-89.8]	78.0 [65.4-90.7]	76.3 [62.8-89.8]	77.2 [67.9-86.45]
Peripheral bile duct dilatation	80.5 [68.4-92.6]	84.2 [72.6-95.8]	84.6 [73.3-95.9]	80.0 [67.6-92.4]	82.3 [73.9-90.7]
Proximal bile duct enhancement	47.5 [32.0-62.9]	86.8 [76.1-97.6]	79.1 [62.9-95.4]	61.1 [48.1-74.1]	65.8 [55.3-76.3]
Extrahepatic spreading	41.4 [26.4-56.5]	92.1 [83.5-100.7]	85 [69.4-100.6]	59.3 [46.8-71.9]	65.8 [55.3-76.3]
Regional lymph node enlargement	56.1 [40.9-71.3]	86.8 [76.1-97.6]	82.1 [67.96-96.3]	64.7 [51.6-77.8]	70.9 [60.9-80.9]
Adjacent organ invasion	34.1 [19.6-48.7]	92.1 [83.5-100.7]	82.3 [64.2-100.5]	56.5 [44.1-68.8]	62.0 [51.2-72.7]
Quantitative variables					
Optimal ERPV (cut-off 0.72)	48.8 [32.9-64.9]	73.7 [56.9-86.6]	66.7 [51.9-78.8]	57.1 [48.3-65.5]	60.8 [49.1-71.6]
Optimal ERD (cut-off 0.79)	51.2 [35.1-67.1]	71.1 [54.1-84.6]	65.6 [51.6-77.3]	57.4 [48.2-66.2]	60.8 [49.1-71.6]

Values are expressed as a percentage [95% confident interval]
IHMCC=intrahepatic mass-forming cholangiocarcinoma, CT=computed tomography, PPV=positive predictive value, NPV=negative predictive value, ERPV=enhancement ratio on the portal venous phase, ERD=enhancement ratio on the delayed phase

Discussion

The imaging findings of IHMCC and CRLM on CT scans have many similarities. Therefore, our study aimed to identify the quantitative methods for differentiating these 2 types of liver tumors. We hypothesized that establishing a formula for quantitative techniques would be beneficial, particularly given that delayed enhancement is a common imaging characteristic of cholangiocarcinoma[8,11,21]. The enhancement ratio on PVP and the delayed 5-minute phase exhibited a statistically significant difference between the IHMCC and CRLM groups, serving as predictors of IHMCC with odds ratios of 2.67 and 2.58, respectively. Upon employing multivariate analysis, ERD remained a significant predictor for IHMCC. This finding could be valuable in differentiating IHMCC from CRLM, particularly in regions with a high prevalence of cholangiocarcinoma. In a previous study by Li et al.[17], dynamic contrast-enhanced magnetic resonance imaging (MRI) was utilized to distinguish peripheral cholangiocarcinoma from other hepatic hypovascular nodules in the early stages. They observed that cholangiocarcinoma exhibited a greater enhancing area than other nodules, including hypovascular metastases, on

both the PVP and delayed phase. These findings support our results indicating that IHMCC demonstrates higher ERPV and ERD. The mean ERD value in IHMCC (0.92) was higher than in CRLM (0.64), aligning with a previous study that identified the most common enhancement pattern of IHMCC as a progressive centripetal enhancement from the venous to the delayed phase[22]. This finding likely correlates with the presence of abundant fibrosis in the center of IHMCC, while the periphery contains more proliferating tumoral cells, as observed in the histopathology[23]. The varying degrees of fibrosis in the center of IHMCC are responsible for the centripetal progressive enhancement[24]. While in CRLM, histopathology typically shows tumor glands surrounded by fibrous stroma. Central acinar necrosis is often present due to tumor hypoxia resulting from an insufficient blood supply[16]. Although ERD was statistically significant in multivariate analysis, its sensitivity was only 51.2%. Its accuracy (60.8%) was lower compared to the qualitative findings, as presented in Table 5. However, its high specificity (71%) greatly aids in distinguishing IHMCC from CRLM, particularly when combined with other qualitative findings. As demonstrated in Figure 4, the presence of an irregular-margin mass with peripheral bile duct dilatation, vascular invasion, and enlarged regional lymph nodes may raise suspicion for IHMCC; however, an ERD below the cut-off of 0.79 may help in distinguishing CRLM from IHMCC.

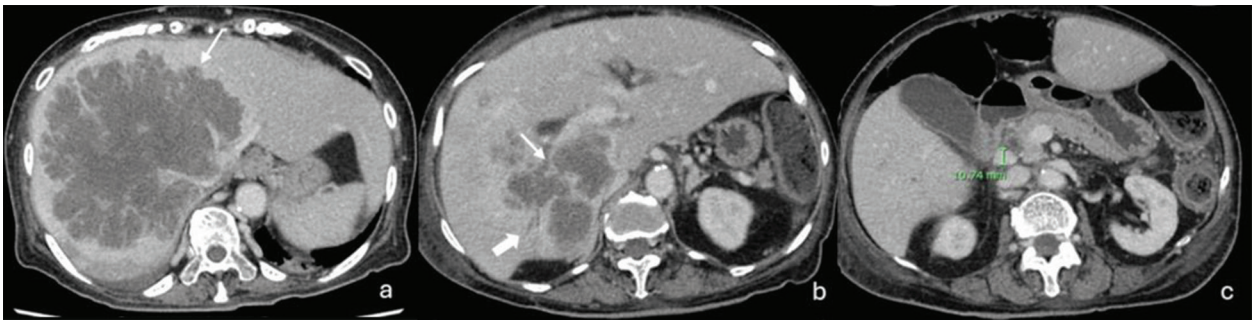

ERPV=enhancement ratio on the portal venous phase, ERD=enhancement ratio on the delayed phase

Figure 4 A case of 70-year-old female with pathological diagnosis of colorectal liver metastasis, moderately differentiated adenocarcinoma. (a) Axial contrast-enhanced computed tomography on the portovenous phase shows large peripheral-enhancing, hypodense mass with irregular border (arrow) mainly in the right hepatic lobe. There is no satellite lesion. (b) The lower level shows peripheral bile duct dilatation distal to the tumor (thick arrow) and right portal vein encasement causing luminal narrowing (thin arrow). (c) There is an enlarged regional lymph node, about 1.1 cm in short axis. These findings were seen more often in intrahepatic mass-forming cholangiocarcinoma. However, the ERPV was 0.52 and the ERD was 0.61, which is less than the optimal cut-off for intrahepatic mass-forming cholangiocarcinoma

Additionally, the mean tumor size of IHMCC was significantly larger than that of CRLM, which may be related to the disease's pathophysiology. IHMCC patients might not exhibit clinical symptoms in the early stages, leading them to seek medical attention only after the disease has progressed[25]. Furthermore, patients with colorectal cancer undergo regular imaging monitoring, potentially resulting in the detection of smaller lesions at the time of diagnosis.

For qualitative analysis, many predictors were found significant for IHMCC in univariate analysis, including size, satellite lesions, location in the right hepatic lobe, hepatic capsular retraction, peripheral bile duct dilatation, proximal bile duct enhancement, vascular invasion, extrahepatic spreading, regional lymph node enlargement, and adjacent organ invasion. However, only peripheral bile duct dilatation and regional lymph node enlargement remained significant in multivariate analysis. From the study by Kovac et al.[26], hepatic capsular retraction and segmental biliary dilatation were identified as significant morphologic features based on multivariate analysis. Additionally, lesion size greater than 5 cm and a lobulated shape were significant findings associated with IHMCC, according to univariate analysis. A previous study by Apisarnthanarak et al.[15] regarding CT appearance for distinguishing between these 2 diseases indicated that peripheral bile duct dilatation, extrahepatic spreading, and proximal bile duct enhancement were the sole predictors in multivariate analysis, supporting our finding of peripheral bile duct dilatation. Although satellite lesions showed statistical significance in predicting IHMCC in univariate analysis and exhibited the highest accuracy and specificity on diagnostic tests in this study, they couldn't be analyzed in multivariate analysis due to being a subgroup finding only in patients with multiple lesions, which could potentially affect accuracy. The results of our study align with those of Shen et al.[27], which aimed to distinguish IHMCC from solitary CRLM based on MRI features. Shen et al. demonstrated that the absence of hepatic capsular retraction and upper abdominal lymphadenopathy increased the diagnostic probability of CRLM. Additionally, irregular hepatic tumor margins were a significant finding in both studies, indicating IHMCC in univariate analysis. However, vascular invasion emerged as a significant finding in our study, in contrast to Shen et al.'s findings.

The strength of our study lies in the utilization of both clinical and pathological diagnoses, which help mitigate diagnostic uncertainty. However, we acknowledge several limitations. Due to the retrospective nature of the study, there were variations in CT scanners and methods, potentially impacting quantitative analysis. Additionally, our cohort comprised a relatively small number of patients from a single center, limiting generalizability. Therefore, for optimal quantitative analysis results, a prospective study involving multiple centers, and a larger patient cohort would be warranted in future research. Furthermore, due to the study design, both readers were aware that all the participants belonged to 1 of the 2 groups, even if they were unaware of the final diagnosis. In the future, comparing hypovascular liver lesions could be beneficial in assisting radiologists in order to improve diagnostic accuracy.

In conclusion, 3 CT characteristics, both qualitative and quantitative, including peripheral bile duct dilatation, regional lymph node enlargement, and ERD, collectively suggest a diagnosis of IHMCC. While the accuracy of ERD alone may be lower compared to the other qualitative findings, when interpreted alongside other qualitative findings, it can contribute to increased specificity for IHMCC.

Funding sources

The authors state that this work has not received any funding.

Conflict of interest

There are no conflicts of interest to declare.

References

1. Banales JM, Marin JJG, Lamarca A, Rodrigues PM, Khan SA, Roberts LR, et al. Cholangiocarcinoma 2020: the next horizon in mechanisms and management. Nat Rev Gastroenterol Hepatol 2020;17:557–88.
2. Gopal P, Robert ME, Zhang X. Cholangiocarcinoma: pathologic and molecular classification in the era of precision medicine. Arch Pathol Lab Med 2023;148:359–70.
3. Florio AA, Ferlay J, Znaor A, Ruggieri D, Alvarez CS, Laversanne M, et al. Global trends in intrahepatic and extrahepatic cholangiocarcinoma incidence from 1993 to 2012. Cancer 2020;126:2666–78.
4. Kirstein MM, Vogel A. Epidemiology and risk factors of cholangiocarcinoma. Visc Med 2016;32:395–400.
5. Sripa B, Pairojkul C. Cholangiocarcinoma: lessons from Thailand. Curr Opin Gastroenterol 2008;24:349–56.
6. Chansitthichok S, Chamnan P, Sarkhampee P, Lertsawatvicha N, Voravisutthikul P, Wattanarath P. Survival of patients with cholangiocarcinoma receiving surgical treatment in an o. viverrini endemic area in Thailand: a retrospective cohort study. Asian Pac J Cancer Prev 2020;21:903–9.
7. Gore RM, Pickhardt PJ, Mortele KJ, Fishman EK, Horowitz JM, Fimmel CJ, et al. Management of incidental liver lesions on CT: a white paper of the ACR incidental findings committee. J Am Coll Radiol 2017;14:1429–37.
8. Fábrega-Foster K, Ghasabeh MA, Pawlik TM, Kamel IR. Multimodality imaging of intrahepatic cholangiocarcinoma. Hepatobiliary Surg Nutr 2017;6:67–78.
9. Olthof SC, Othman A, Clasen S, Schraml C, Nikolaou K, Bongers M. Imaging of Cholangiocarcinoma. Visc Med 2016;32:402–10.
10. Venkatesh SK, Chandan V, Roberts LR. Liver masses: a clinical, radiologic, and pathologic perspective. Clin Gastroenterol Hepatol 2014;12:1414–29.
11. Mendiratta-Lala M, Park H, Kolicaj N, Mendiratta V, Bassi D. Small intrahepatic peripheral cholangiocarcinomas as mimics of hepatocellular carcinoma in multiphasic CT. Abdom Radiol (NY) 2017;42:171–8.
12. Kow AWC. Hepatic metastasis from colorectal cancer. J Gastrointest Oncol 2019;10:1274–98.
13. Schima W, Kulinna C, Langenberger H, Ba-Ssalamah A. Liver metastases of colorectal cancer: US, CT or MR? Cancer Imaging 2005;5:S149–56.
14. Valderrama-Treviño AI, Barrera-Mera B, Ceballos-Villalva JC, Montalvo-Javé EE. Hepatic Metastasis from Colorectal Cancer. Euroasian J Hepatogastroenterol 2017;7:166–75.
15. Apisarnthanarak P, Pansri C, Maungsomboon K, Thamtorawat S. The CT appearances for differentiating of peripheral, mass-forming cholangiocarcinoma and liver meatastases from colorectal adenocarcinoma. J Med Assoc Thai 2014;97:415–22.
16. Paulatto L, Dioguardi Burgio M, Sartoris R, Beaufrère A, Cauchy F, Paradis V, et al. Colorectal liver metastases: radiopathological correlation. Insights Imaging 2020;11:99.
17. Li S, Qian H, Peng Y, Jia H, Lin G. Differentiating peripheral cholangiocarcinoma in stages T1N0M0 and T2N0M0 from hepatic hypovascular nodules using dynamic contrast-enhanced MRI. Sci Rep 2017;7:8084.
18. King MJ, Hectors S, Lee KM, Omidele O, Babb JS, Schwartz M, et al. Outcomes assessment in intrahepatic cholangiocarcinoma using qualitative and quantitative imaging features. Cancer Imaging 2020;20:43.
19. Landis JR, Koch GG. The measurement of observer agreement for categorical data. Biometrics 1977;33:159–74.
20. Cicchetti DV. Guidelines, criteria, and rules of thumb for evaluating normed and standardized assessment instruments in psychology. Psychol Assess 1994;6:284–90.
21. Seo N, Kim DY, Choi JY. Cross-Sectional Imaging of Intrahepatic Cholangiocarcinoma: Development, Growth, Spread, and Prognosis. AJR Am J Roentgenol 2017;209:W64–75.22.
22. Chen Y, Pan Y, Shen KR, Zhu XL, Lu CY, Li QH, et al. Contrast-enhanced multiple-phase imaging features of intrahepatic mass-forming cholangiocarcinoma and hepatocellular carcinoma with cirrhosis: a comparative study. Oncol Lett 2017;14:4213–9.
23. Vijgen S, Terris B, Rubbia-Brandt L. Pathology of intrahepatic cholangiocarcinoma. Hepatobiliary Surg Nutr 2017;6:22–34.
24. Chung YE, Kim MJ, Park YN, Choi JY, Pyo JY, Kim YC, et al. Varying appearances of cholangiocarcinoma: radiologic-pathologic correlation. Radiographics 2009;29:683–700.
25. El-Diwany R, Pawlik TM, Ejaz A. Intrahepatic Cholangiocarcinoma. Surg Oncol Clin N Am 2019;28:587–99.
26. Kovač JD, Galun D, Đurić-Stefanović A, Lilić G, Vasin D, Lazić L, et al. Intrahepatic mass-forming cholangiocarcinoma and solitary hypovascular liver metastases: is the differential diagnosis using diffusion-weighted MRI possible? Acta Radiol 2017;58:1417–26.

27. Shen K, Mo W, Wang X, Shi D, Qian W, Sun J, et al. A convenient scoring system to distinguish intrahepatic mass-forming cholangiocarcinoma from solitary colorectal liver metastasis based on magnetic resonance imaging features. Eur Radiol 2023;33:8986–98.